

Adsorption of Synthetic Cationic Polymers on Model Phospholipid Membranes: Insight from Atomic-Scale Molecular Dynamics Simulations

Andrei Yu. Kostritskii,[†] Diana A. Kondinskaia,[†] Alexey M. Nesterenko,[‡] and Andrey A. Gurtovenko^{*,†,§}

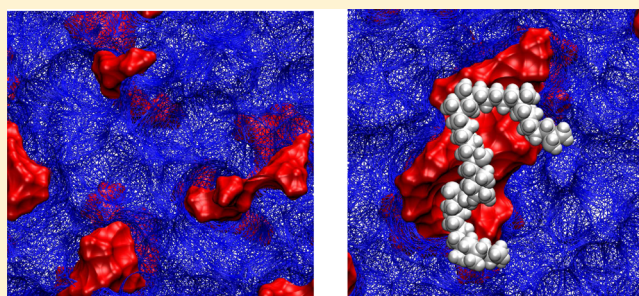
[†]Faculty of Physics, St. Petersburg State University, Ulyanovskaya str. 3, Petrodvorets, St. Petersburg 198504 Russia

[‡]Belozersky Institute of Physico-Chemical Biology, Lomonosov Moscow State University, Moscow 119991 Russia

[§]Institute of Macromolecular Compounds, Russian Academy of Sciences, Bolshoi Prospect V.O. 31, St. Petersburg 199004 Russia

Supporting Information

ABSTRACT: Although synthetic cationic polymers represent a promising class of effective antibacterial agents, the molecular mechanisms behind their antimicrobial activity remain poorly understood. To this end, we employ atomic-scale molecular dynamics simulations to explore adsorption of several linear cationic polymers of different chemical structure and protonation (polyallylamine (PAA), polyethylenimine (PEI), polyvinylamine (PVA), and poly-L-lysine (PLL)) on model bacterial membranes (4:1 mixture of zwitterionic phosphatidylethanolamine (PE) and anionic phosphatidylglycerol (PG) lipids). Overall, our findings show that binding of polycations to the anionic membrane surface effectively neutralizes its charge, leading to the reorientation of water molecules close to the lipid/water interface and to the partial release of counterions to the water phase. In certain cases, one has even an overcharging of the membrane, which was shown to be a cooperative effect of polymer charges and lipid counterions. Protonated amine groups of polycations are found to interact preferably with head groups of anionic lipids, giving rise to formation of hydrogen bonds and to a noticeable lateral immobilization of the lipids. While all the above findings are mostly defined by the overall charge of a polymer, we found that the polymer architecture also matters. In particular, PVA and PEI are able to accumulate anionic PG lipids on the membrane surface, leading to lipid segregation. In turn, PLL whose charge twice exceeds charges of PVA/PEI does not induce such lipid segregation due to its considerably less compact architecture and relatively long side chains. We also show that partitioning of a polycation into the lipid/water interface is an interplay between its protonation level (the overall charge) and hydrophobicity of the backbone. Therefore, a possible strategy in creating highly efficient antimicrobial polymeric agents could be in tuning these polycation's properties through proper combination of protonated and hydrophobic blocks.



INTRODUCTION

Polymeric biocides (i.e., polymers with antimicrobial activity) represent an important class of antibacterial agents.^{1,2} They have shown a considerable potential for application in such areas as antimicrobial therapy and coatings (sterile bandages and clothing),^{3,4} food preservation, and water and soil sterilization.^{1,5} Polymeric biocides have many advantages over low-molecular-weight agents as they demonstrate lower toxicity,^{6,7} long-term antibacterial ability, biocidal activity to a broader range of pathogenic organisms^{1,8} and drug-resistant bacteria.⁹ Furthermore, their chemical stability and reduced volatility allow one to minimize negative effects of such factors as photolytic decomposition and transportation.

Synthetic cationic polymers constitute a wide and important class of polymeric biocides. A great variety of cationic polymers that differ in their chemical structure, size, charge density, and type of ionogenic groups has been synthesized and tested against their antimicrobial activity.^{1,2} In particular, cationic polymers with pendant biguanide groups¹⁰ and polymeric

phosphonium salts¹¹ were shown to bind to the surface of bacterial cells to a greater extent as compared to low-molecular weight cations due to a higher positive charge density of the polymers. Polyethylenimine (PEI), a cationic polymer with one of the highest charge density among linear polycations, was found to make Gram-negative bacteria (such as *E. coli*) permeable to hydrophobic antibiotics;¹² its alkylated derivatives displayed biocidal action also against *S. aureus*.¹³ Panarin et al.¹⁴ studied interactions of bacterial cells with water-soluble cationic polymers based on vinylamine, aminoalkyl methacrylates, and their quaternary ammonium salts and showed that the polymers changed the permeability of bacterial membranes, increased transport of low-molecular weight substances into cells and suppressed some of bacterial enzymes. A more recent study demonstrated that polyvinylamine (PVA) and alkylated PVA

Received: July 13, 2016

Revised: September 15, 2016

Published: September 19, 2016

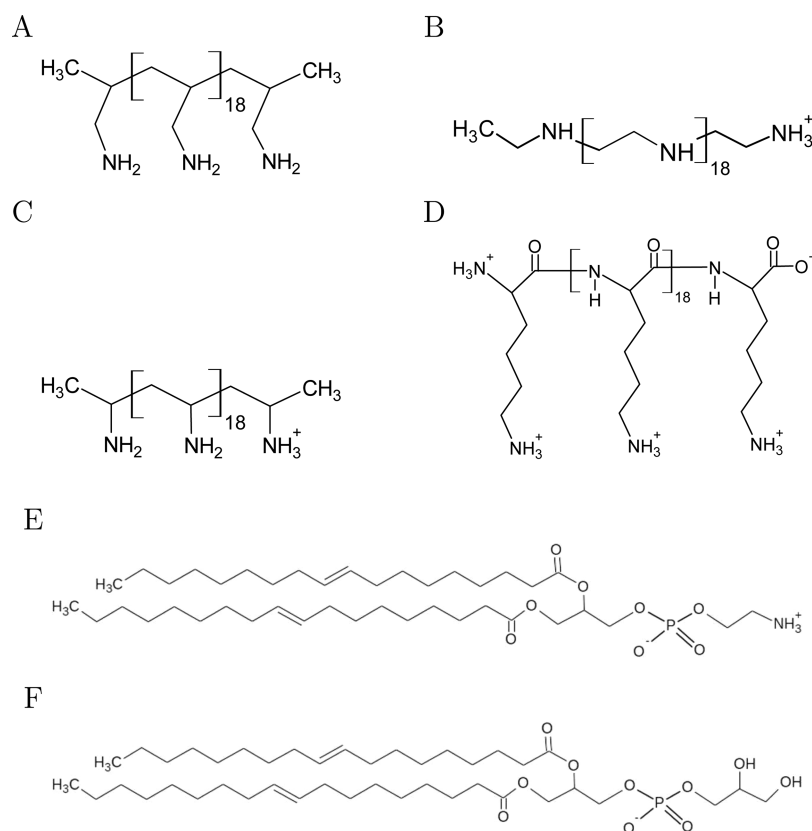


Figure 1. Chemical structures of polycations (A–D) and phospholipids (E,F) studied. (A) Polyallylamine, PAA, (B) polyethylenimine, PEI, (C) polyvinylamine, PVA, (D) poly-L-lysine, PLL, (E) dioleoylphosphatidylethanolamine, DOPE, and (F) dioleoylphosphatidylglycerol, DOPG.

derivatives were able to inhibit the growth of both Gram-positive and Gram-negative bacteria.^{15,16} Polyallylamine (PAA), another polycation with ionogenic primary amino groups, was also studied with respect to its antibacterial activity in solution and was found to inhibit the growth of both *E. coli* and *S. aureus*.¹⁷ Furthermore, layer-by-layer deposition of PAA also displayed considerable antimicrobial activity.¹⁸ As far as cytolytic and antimicrobial polypeptides are concerned, poly-L-Lysine (PLL) is often considered as an important representative.^{19–23}

According to ref 10, a mechanism of action of cationic biocides can be summarized as follows. After adsorption on the surface of a bacterial cell, a biocide diffuses through the cell wall toward the cytoplasmic membrane, binds to it, and induces rupture of the membrane, giving rise to release of cytoplasmic constituents and eventually to cell death. As a primary target for cationic polymers is the cytoplasmic membrane of bacterial cells,^{2,5,10,24} it comes as no surprise that the impact of polycations on model membranes of various composition has been studied extensively both experimentally²⁵ and computationally.²⁶ In particular, Ikeda et al. demonstrated that cationic polymers had almost no effect on membranes composed of zwitterionic (neutral) phosphatidylcholine (PC) and phosphatidylethanolamine (PE) lipids, while they interacted strongly with anionic pure phosphatidylglycerol (PG) and mixed PG/PE lipid membranes, inducing aggregation of the anionic lipids in the vicinity of the adsorption site and reducing the phase transition temperature of PG lipids.^{27,28} Such formation of domains enriched with anionic lipids upon adsorption of cationic polymers onto lipid vesicles was also reported in a number of studies.^{29–34} It is noteworthy that the polymer

topology and molecular weight are also among the factors that affect polycation–membrane interactions. For instance, it was shown that short PLL fragments destabilize lipid membranes, while longer PLL molecules are able to demonstrate an opposite effect, i.e., increase the membrane stability.^{32,33} Another related study focused on the effects of PAA, PEI and PLL and showed that only PAA and branched PEI are capable of changing the permeability of anionic membranes built from PC and phosphatidylserine (PS) lipids.³⁵

In addition to experimental studies, computer modeling is normally considered as a source of important information that is not accessible easily through any other techniques. This is essentially the case for atomistic computer simulations that are able to provide an unprecedented microscopic insight into the structure and properties of molecular systems in question. As far as synthetic cationic polymers are concerned, the vast majority of computational studies have focused on dendrimers, a special class of hyperbranched polymers that are able to carry a large positive charge under physiological conditions; see ref 36 for a recent review. Considerably less attention has been paid to linear cationic polymers and their interactions with model biological membranes. In fact, the related studies in which atomistic computer simulations were applied to polycation-membrane systems appeared only very recently.²⁶

Kepczynski et al.³⁷ considered the effect of a cationic polymer poly(allyl-*N,N*-dimethyl-*N*-hexylammonium chloride) on a zwitterionic palmitoyl-oleoyl-phosphatidylcholine (POPC) lipid bilayer. It was shown that short fragments of the polycation, being placed inside the bilayer, are able to enhance the permeability of the bilayer through formation of hydrophilic pores filled with water. Hill and co-workers^{38,39} employed

atomistic molecular dynamics simulations to study a possible mechanism of disruption of a model bacterial membrane by cationic polymer oligo-*p*-phenylene ethynylenes (OPEs). A mixed dioleoylphosphatidylethanolamine (DOPE)/dioleoylphosphatidylglycerol (DOPG) lipid bilayer was used as a model of bacterial membranes. The authors showed that a polycation, being placed in the water phase, adsorbs on the surface of a lipid bilayer and interacts preferentially with anionic DOPG lipids, giving rise to formation of DOPG-rich domains. However, a considerable bilayer perturbation accompanied by water pore formation was observed only in the case when a polycation is inserted in the interior of a bilayer. Choudhury et al.⁴⁰ studied the impact of linear polyethylenimine (PEI) in different protonation states on a zwitterionic DOPC lipid bilayer. Similar to the above-mentioned studies, the authors demonstrated that protonated PEI was able to induce formation of a water pore when it was inserted inside the bilayer perpendicular to the bilayer surface. Finally, Lorenz et al.⁴¹ studied adsorption of a short polylysine chain on mixed anionic/zwitterionic lipid bilayers and highlighted the importance of hydrogen bonds that stabilized the polycation-membrane complexes.

It should be emphasized that existing computational studies of polycation-bilayer systems reported partial disruption of the bilayer structure via formation of transmembrane water pores when simulations started from an essentially nonequilibrium state, namely, when a highly charged linear polymer was inserted into the bilayer interior. As a result, a molecular mechanism of pore formation resembles the one highlighted in ref 42: introduction of charges into the hydrophobic lipid core of a membrane leads to reorientation of lipid head groups toward the charges and to the appearance of water defects (water molecules) in the bilayer interior to hydrate these charged groups. Note that a complete sequence of events, from adsorption from solution via insertion into the bilayer interior to eventually pore formation, is currently beyond the time scales accessible through atomistic molecular dynamics simulations. While computational studies have focused mainly on cation-induced pore formation, considerably less attention has been paid to the initial steps of polycation's action on biological membranes. Therefore, here we present a first systematic study of adsorption of various linear cationic polymers from aqueous solution on model bacterial membranes. We chose to consider the following four linear polycations: polyallylamine (PAA), polyethylenimine (PEI), polyvinylamine (PVA), and poly-L-lysine (PLL); see Figure 1 for the polycations' chemical structures. These polymers differ in the chemical structure of their monomer units and - through the structural difference - in the protonation state at physiological conditions. The use of the state-of-the-art molecular dynamics simulations allows us to follow closely polymer's adsorption on the membrane surface and subsequent rearrangement of water molecules, counterions, and lipid molecules within the lipid/water interface at an atomic scale.

METHODS AND MODELS

We have performed atomistic molecular dynamics simulations of a model phospholipid membrane in the presence of synthetic cationic polymers. A membrane consists of a 4:1 mixture of zwitterionic dioleoylphosphatidylethanolamine (DOPE) and anionic dioleoylphosphatidylglycerol (DOPG) lipids, see Figure 1 for lipids' chemical structures. Such a mixture mimics closely the lipid composition of the inner membrane of Gram-negative bacteria⁴³ and has been considered

in a number of experimental and simulation studies.^{38,39,44,45} A PE/PG membrane consisted of 128 lipid molecules (51 DOPE and 13 DOPG lipids per leaflet). A polycation (or polycations) was placed in the vicinity of one of the membrane leaflets. Four linear polycations were considered: polyallylamine (PAA), polyethylenimine (PEI), polyvinylamine (PVA), and poly-L-lysine (PLL); see Figure 1 for polymer's chemical structures. All the polycations consisted of 20 repeating monomer units; their protonation states were adjusted to match the physiological conditions (pH \approx 7). Based on experimental data, the protonation level was set to 15%, 50%, 50%, and 100% for PAA,⁴⁶ PEI,⁴⁷ PVA,⁴⁸ and PLL,⁴⁸ respectively (this was achieved through protonating correspondingly 3, 10, 10, and 20 amine groups of a polymer). Each system was solvated with an excess of water, and the number of water molecules varied from \sim 7700 to 10 900 depending on the type of a polycation and its concentration. Correspondingly, the total number of atoms in the systems was in the range from \sim 40 000 to 48 000. An appropriate number of counterions (Na^+ ion for a mixed PE/PG membrane and Cl^- ions for polycations) were added in the system to achieve electroneutrality. A list of simulated "membrane-polycation" systems is presented in Table 1.

Table 1. Simulated Membrane-Polycation Systems

system	polycation	no. of polycations	total charge of polycation(s) (e)	simulation time (ns)
Lipid-0				500
Lipid-PAA	PAA	1	+3	700
Lipid-PEI	PEI	1	+10	700
Lipid-PVA	PVA	1	+10	700
Lipid-PLL	PLL	1	+20	1000
Lipid-PAA \times 3	PAA	3	+9	700
Lipid-PEI \times 2	PEI	2	+20	700
Lipid-PVA \times 2	PVA	2	+20	700

A recently developed AMBER-based force-field Slipids^{49–51} was used for DOPE and DOPG lipids. Parameters for monovalent ions were taken from ref 52, and the TIP3P model⁵³ was used to describe water. The AMBER99 force-field^{54,55} was used for polycations. As it contains a full set of parameters only for PLL, partial charges of PAA, PVA, and PEI were taken from ref 56.

All simulations were carried out in the NPT ensemble at $T = 310$ K and $P = 1$ bar with use of the GROMACS 4.5.6 software.⁵⁷ Pressure was controlled semiisotropically and the thermostat was applied separately to a lipid membrane, polycation(s), and a water bath with ions. The Berendsen scheme⁵⁸ was used for both thermostat and barostat during equilibration. For production runs the Nose-Hoover thermostat^{59,60} and the Parrinello-Rahman barostat⁶¹ were applied. All bonds were constrained with the LINCS algorithm.⁶² The time step was 2 fs. Lennard-Jones interactions were cut off at 1.4 nm, while the particle-mesh Ewald method⁶³ was used to handle electrostatic interactions. The VMD package⁶⁴ was used for visualization.

Prior actual "membrane-polycation" simulations a PE/PG lipid membrane and polycations were separately pre-equilibrated in aqueous solution for 100 and 50 ns, respectively. The simulation of the polycation-free membrane system Lipid-0 was extended for more 400 ns, see Table 1. From the simulations of polycations we calculated their radii of gyration (0.9 ± 0.1 , 1.2 ± 0.1 , 1.0 ± 0.1 , and 1.4 ± 0.1 nm for PAA, PEI, PVA, and PLL, respectively) and end-to-end distances (2.1 ± 0.7 , 3.1 ± 0.7 , 2.9 ± 0.7 , and 2.8 ± 0.7 nm for PAA, PEI, PVA, and PLL, respectively). These data guided us in setting up simulations of "polycation-membrane" systems in such a way that polycations did not interact with their periodic images. The initial configurations of the systems were prepared as follows. A pre-equilibrated lipid membrane was placed in a simulation box asymmetrically with respect to the center of the box along the direction of the membrane normal. This allowed one to put more water molecules on the membrane side that was in contact with a polycation. The box size in the membrane plane was set to (6.38 nm \times 6.38 nm) in all systems, while the box dimension along the membrane

normal varied from 10 to 12.5 nm. A well-equilibrated polycation molecule was rotated to make its long axis parallel to the membrane surface. A polycation was then placed nearby the membrane leaflet with the distance between the nearest polycation's atom and the lipid leaflet being ~ 1.5 nm along the membrane normal. In turn, the distance between a polycation and the end of a simulation box was between 1.5 and 2.5 nm, excluding thereby unwanted jumps of the polymer to the opposite side of a box. After that a short run (100 ps) with position restraints on a polycation was carried out. A polycation was then released and the simulations continued for 700 ns for systems with PAA, PEI and PVA. As PLL required longer time for proper equilibration on the membrane surface, the corresponding simulation was extended to 1 μ s; see Table 1. The simulation protocol was the same also for systems with multiple polymer chains. All average values presented throughout the paper were calculated by averaging over last 600 ns (membrane systems with polycations) and 400 ns (the pure membrane system Lipid-0) of MD trajectories. The overall simulation time amounted to ~ 6 μ s.

The bulk ionic concentration was measured for each system as the average concentration of Cl^- and Na^+ ions at the most distant position from both membrane surfaces in a simulation box (the averaging was carried out over last 300 ns of MD trajectories). The surface potential Ψ_s was estimated as a potential of mean force through the following equation:

$$\Psi_s = \frac{RT}{zF} \ln \frac{C_{\text{bulk}}}{C_0}$$

where z is a charge of a counterion, C_{bulk} is the bulk concentration of counterions, and C_0 is the concentration of counterions at the outer Helmholtz plane. The outer Helmholtz plane separates the diffuse layer of an electrical double layer and the surface; its location was defined as a position of the maximum of the density profile of counterions that are not able to permeate into the membrane (Cl^- ions).⁶⁵ We note that the lipid membrane surface is rough,⁶⁶ so that introducing any ideal plane represents a simplification. Such an approach is necessary here for formulating solvable equations. The values of C_{bulk} and Ψ_s and the positions of the outer Helmholtz plane are presented in Table 2.

Table 2. Bulk Ion Concentration, Surface Potential, and Position the Outer Helmholtz Plane for All Simulated Systems

system	C_{bulk} (mM)	Helmholtz plane (nm) ^a	Ψ_s [polymer] (mV) ^b	Ψ_s [ref] (mV) ^c
Lipid-0	37	2.66	-17	-17
Lipid-PAA	45	2.66	-18	-23
Lipid-PEI	88	2.76	+7	-19
Lipid-PVA	77	2.76	+5	-20
Lipid-PLL	101	3.16	+26	-16
Lipid-PAA $\times 3$	59	2.66	0	-24
Lipid-PEI $\times 2$	96	2.76	+26	-17
Lipid-PVA $\times 2$	90	2.66	+29	-20

^aThe position of the outer Helmholtz plane on the membrane side that is in contact with polycation(s). The corresponding location of the outer Helmholtz plane on the polymer-free side of a membrane was set to 2.66 nm for all systems. ^bThe surface potential on the membrane side that is in contact with polycation(s). ^cThe reference surface potential on the polymer-free membrane side.

RESULTS AND DISCUSSION

Binding of a Polycation to the Membrane Surface. To explore the process of binding of a polycation on the surface of a model bacterial membrane we evaluated the distance between the centers of mass (COM) of a cationic polymer and a membrane (Figure 2). The overall electric charge of a PE/PG

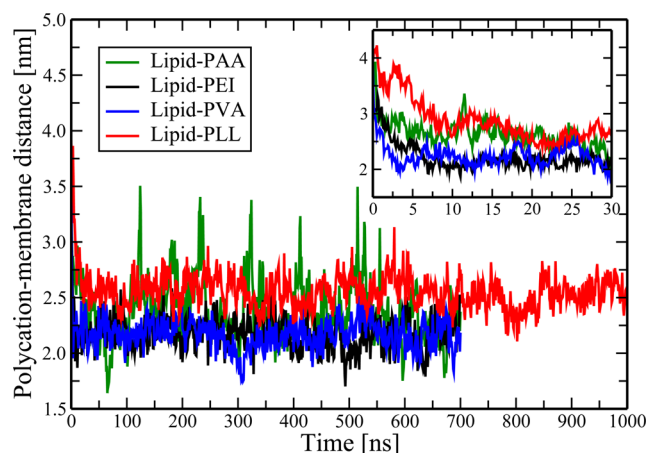


Figure 2. Time evolution of the distance between centers of masses of a polycation and a PE/PG membrane along the membrane normal.

membrane leaflet equals $-13e$, while the charge of polycations varies from $+3e$ to $+20e$ (see Table 1), so that one can expect that adsorption is driven by electrostatic attractive interactions between polymers and the membrane surface. As evident from the inset of Figure 2, the process of polycation's adsorption from the water phase is rather fast for all polymers considered and takes less than 20 ns. Note that our simulations correspond to last stages of polycation adsorption and do not include the mass transfer from bulk water to the membrane surface. In our model systems the initial adsorption is limited by diffusion of a polycation and depends on the distance between closest atoms of a polymer and a membrane in the beginning of simulations (which was set to 1.5 nm for all the membrane-polycation systems considered here). As far as the stability of polycation binding to a PE/PG membrane is concerned, the binding can be considered as stable for all polymers except PAA whose total charge is only $+3e$: as seen from Figure 2, this polymer is able to unbind from the membrane surface for relatively short periods of time and come back. Therefore, the stability of the polymer-membrane binding seems to depend mostly on the total charge of a polycation rather than on its chemical structure. This is typical for any charged surface: a cationic polymer, being the most charged polyion in the electrolyte solution, accumulates at the outer Helmholtz plane regardless its chemical nature. In turn, tight polycation binding that modifies the total charge of the surface is also defined by the ability of the polycation to bind to lipid polar head groups.

While the initial adsorption of a polycation is electrostatically driven and mostly determined by the attractive interactions of polycations with anionic lipids DOPG, once a polycation is on the membrane surface it starts to interact also with zwitterionic lipids DOPE. Both DOPG and DOPE lipids have phosphate groups with negative partial charges, so that zwitterionic lipids can also contribute to the stability of polymer-membrane binding. To get insight into the role of DOPG and DOPE lipids we calculated radial distribution functions (RDF) for phosphorus atoms of the lipids and nitrogen atoms of protonated amine groups of polycations, see Figure 3. It is clearly seen that the main RDF peaks are much higher for DOPG lipids as compared to DOPE counterparts, implying much stronger interactions of DOPG lipids with protonated groups of polymers. Therefore, after the initial binding has taken place, polycations still interact preferably with anionic PG lipids on the PE/PG membrane surface in spite of the fact that

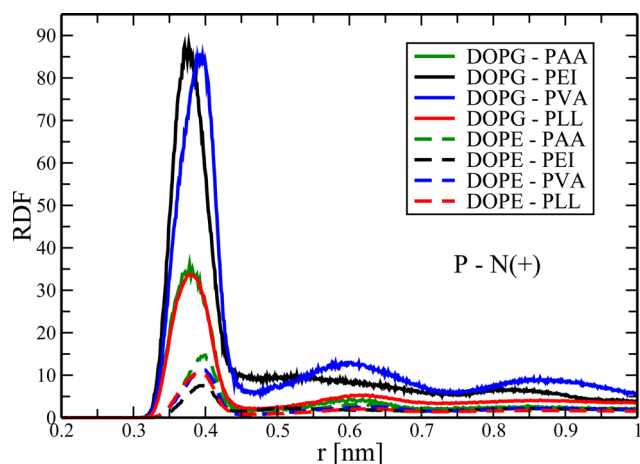


Figure 3. Radial distribution functions of phosphorus atoms of lipid head groups and nitrogen atoms of protonated amine groups of polycations. Shown are results for DOPG and DOPE lipids (solid and dashed lines, respectively).

the number of zwitterionic PE lipids is four times larger than that for anionic ones. This is due to the electrostatically driven accumulation of anionic lipids around oppositely charged groups of a cationic polymer bound to the membrane.

To further characterize the interactions between polycations and anionic DOPG lipids, in Figure 4 (top), we presented the number of contacts between protonated amine groups of polycations and negatively charged phosphate groups of DOPG lipids. To calculate the numbers of contacts, for each polycation, we first identified the radius of the first coordination shell that was defined through a position of the first minimum of the corresponding radial distribution function; see Figure 3. The number of contacts was then calculated as a cumulative number of nitrogen atoms of polymer's protonated amine groups within first coordination shells of phosphate groups of DOPG lipids.^{67,68}

Figure 4 (top) shows several striking features. First, for PAA, the least charged polycation, we see relatively long periods of time (up to 50 ns) when the polymer does not form any contacts with anionic lipids, which again is a sign of very weak and unstable binding of PAA to the membrane surface. Second, for the rest of polycations (PEI, PVA, and PLL) one has approximately the same average numbers of contacts in spite of the differences in overall charges and chemical structures. The average values for the numbers of contacts amount to 1 ± 1 , 7 ± 2 , 6 ± 2 , and 5 ± 2 for PAA, PEI, PVA, and PLL, respectively. Interestingly, for all cationic polymers the average number of contacts with anionic PG lipids is considerably smaller than the number of polymer's protonated amine groups. This effect is most pronounced for PLL: while this polymer has twice as many protonated groups as PEI and PVA, its average number of contacts with anionic PG lipids turns out to be smaller as compared to other two polymers. We note that this is also seen through a relatively small RDF peak for PLL in Figure 3. Given that 13 DOPG lipids in total are available for binding with polycations, such a small average number of PLL-DOPG contacts is a signature of the existence of certain PLL's structural features that prevent tighter binding of the polymer. PLL represents a polypeptide chain with relatively massive side chains; they sterically restrict mutual orientations of lysine residues along the main chain, so that some of PLL's protonated amine groups are forced to stay in the water

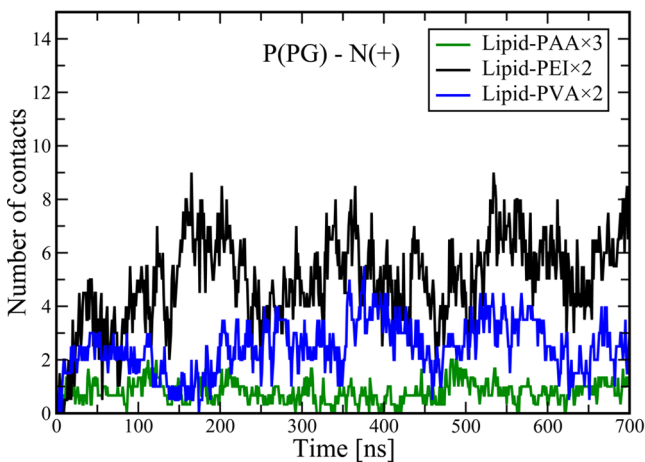
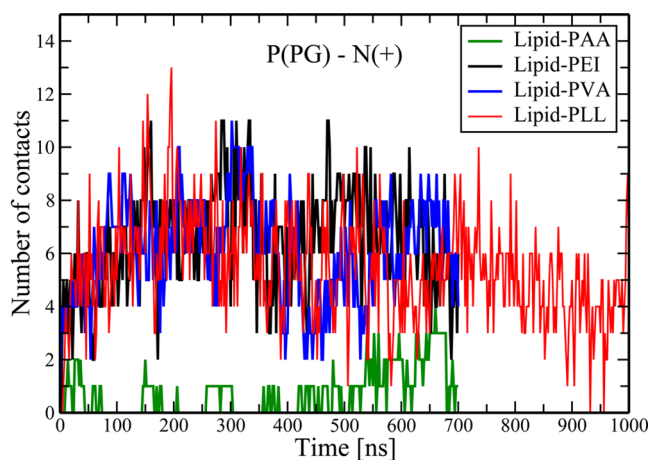


Figure 4. Number of contacts between phosphorus atoms of anionic DOPG lipids and nitrogen atoms of protonated amine groups of polycations as a function of time. Shown are results for the systems with single (top) and multiple (bottom) polymer chains. In the latter case, the number of contacts per chain is shown.

phase without contacts with the membrane surface. It is also noteworthy that polycations' protonated groups that participate in contacts with PG lipid head groups can form more than one contact with anionic lipids as confirmed through the calculation of corresponding coordination numbers: 1.2 ± 0.2 , 1.3 ± 0.2 , and 1.1 ± 0.2 for PEI, PVA, and PLL, respectively.

Finally, we evaluated the average number of hydrogen bonds between protonated amine groups of polycations and phosphate groups of anionic PG lipids: 0.6 ± 0.8 , 5 ± 2 , 5 ± 2 , and 4 ± 2 for PAA, PEI, PVA, and PLL, respectively. Therefore, although the initial attraction between cationic polymers and anionic membranes is electrostatically driven, hydrogen bonds also play a significant role in stabilizing of the "membrane-polycation" complexes.⁴¹

Polycation-Induced Changes in the Lipid/Water Interface. Adsorption of polycations to the anionic membrane surface should inevitably lead to structural changes in the lipid/water interface. These may include reorientation of water molecules close to the membrane surface, release of counterions bound to the surface and changes in lipid packing due to partitioning of the polymer into the lipid/water interface.

The orientation of water molecules close to the membrane surface can be characterized by the angle between the water dipoles and the outward membrane normal. In Figure 5 we

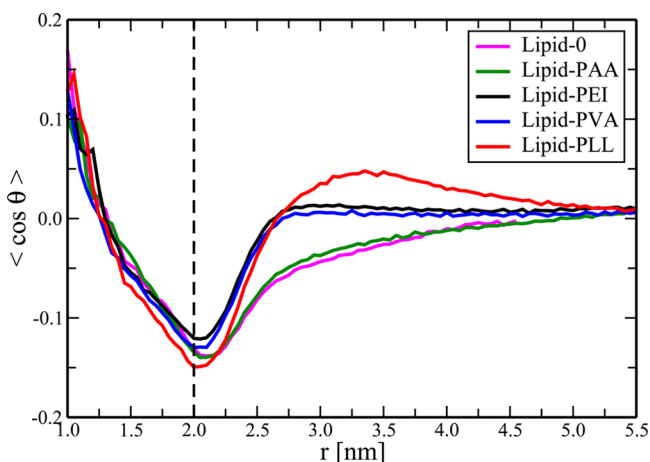


Figure 5. Average cosine of the angle between water dipoles and the outward membrane normal as a function of the distance from the membrane center ($r = 0$). The position of the lipid/water interface is defined as a point where mass density profiles of lipids and water cross and is shown by a vertical dashed line.

present the average cosine of this angle as a function of the distance from the membrane center. When there is no preferential orientation of water molecules, this quantity equals zero as it is the case for bulk water, see Figure 5 for $r > 5.0$ nm. Closer to the lipid/water interface one has negative values of $\langle \cos \theta \rangle$ for the polycation-free system Lipid-0, which implies that hydrogen atoms of water molecules are directed toward the membrane. Such water orientation occurs due to an overall negative surface charge of a mixed PE/PG membrane; this charge cannot be completely screened by sodium counterions that are present in the system.

When a polycation adsorbs on the membrane surface, its effect on water orientation in the interfacial region turns out to depend on polycation's overall charge. In particular, a slightly charged PAA does not affect the orientation of water molecules as compared to a polycation-free system, see Figure 5. In turn, adsorption of PEI and PVA, two polymers of the same charge of $+10e$ leads to a considerable neutralization of the surface charge of an anionic PE/PG membrane: water dipoles stop feeling a negative charge of the membrane (i.e., $\langle \cos \theta \rangle$ becomes zero) at much shorter distances as compared to a polycation-free system. Finally, PLL whose charge exceeds the overall charge of a membrane leaflet ($+20e$) versus ($-13e$), overcharges the PE/PG membrane, so that the average direction of the water dipoles in the lipid/water interface region is inverted ($\langle \cos \theta \rangle$ becomes positive); see Figure 5. Thus, in contrast to monovalent counterions, polycations are able to effectively neutralize and even overcharge the membrane surface.

In Figure 6 (top), we plot mass density profiles of sodium ions for different membrane systems. The peaks in the profiles directly correspond to Na^+ ions that are bound to the lipid/water interface. It is seen that adsorption of all polycations leads to reduction of the height of the peaks, the reduction becomes more pronounced when the overall charge of a polycation increases. In other words, a positive charge of polycations effectively pushes sodium counterions from the membrane surface to the water phase.

To explore the distribution of ions in more detail, in Figure 7, we present the local concentration of sodium and chloride ions as well as protonated amine groups of polymers on both

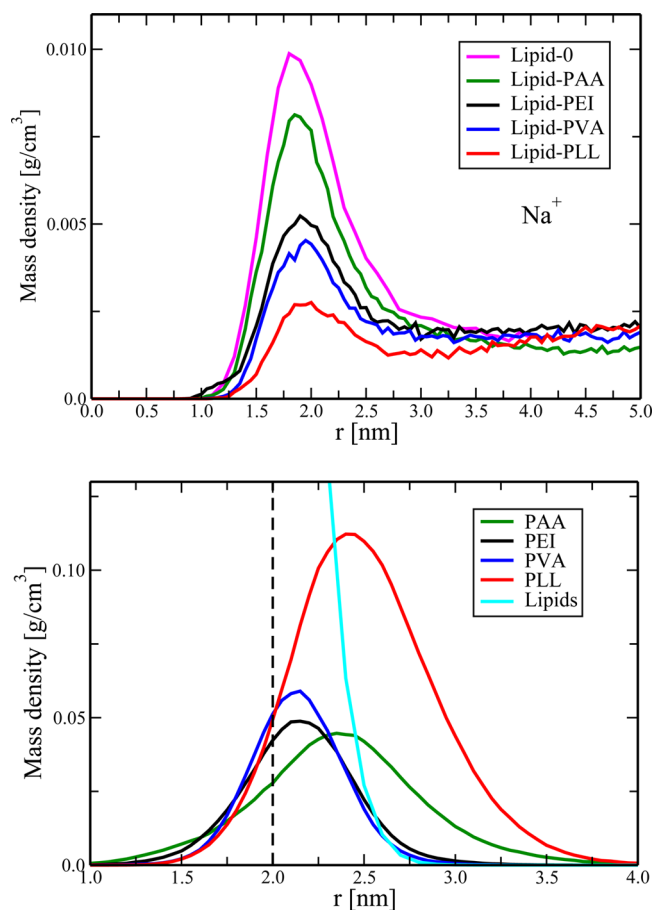


Figure 6. (Top) Mass density profiles of sodium counterions as a function of the distance from the membrane center ($r = 0$). Shown are results for a membrane leaflet that is in contact with a polycation. (Bottom) Component-wise mass density profiles for polycations and lipids as a function of the distance from the membrane center ($r = 0$). The position of the lipid/water interface is shown by a vertical dashed line.

sides of a PE/PG membrane. For the Lipid-PLL system we witness that the concentration of Cl^- ions at the outer Helmholtz plane of the leaflet with PLL exceeds considerably that of Na^+ ions. This is in great contrast to what is observed on the polymer-free leaflet and is a sign of the above-mentioned PLL-induced overcharging of a membrane. It is also noteworthy that the distribution of the protonated amine groups of PLL has two maxima, supporting the fact that not all charged residues of PLL form contacts with the membrane surface. Surprisingly, for the systems with PEI and PVA, the overall charge of ions at the outer Helmholtz plane of leaflets with a polycation is also slightly negative, implying an overcharging of the membrane; see Figure 7. Calculated surface potentials Ψ_s of the corresponding leaflets (see Table 2) turn out to be positive, additionally supporting the overcharging.

This result is nontrivial as the overall charge of the polycations (PEI and PVA) is smaller than that of the PE/PG membrane leaflet ($+10e$ vs $-13e$), so that the polymer alone is not able to neutralize the membrane charge and correspondingly induce the observed overcharging. To explain the effect we applied the Gouy–Chapman–Stern theory to the membrane systems at hand; see the Supporting Information for detailed derivations. This theory was previously used in several studies to relate the ionic composition and the surface potential

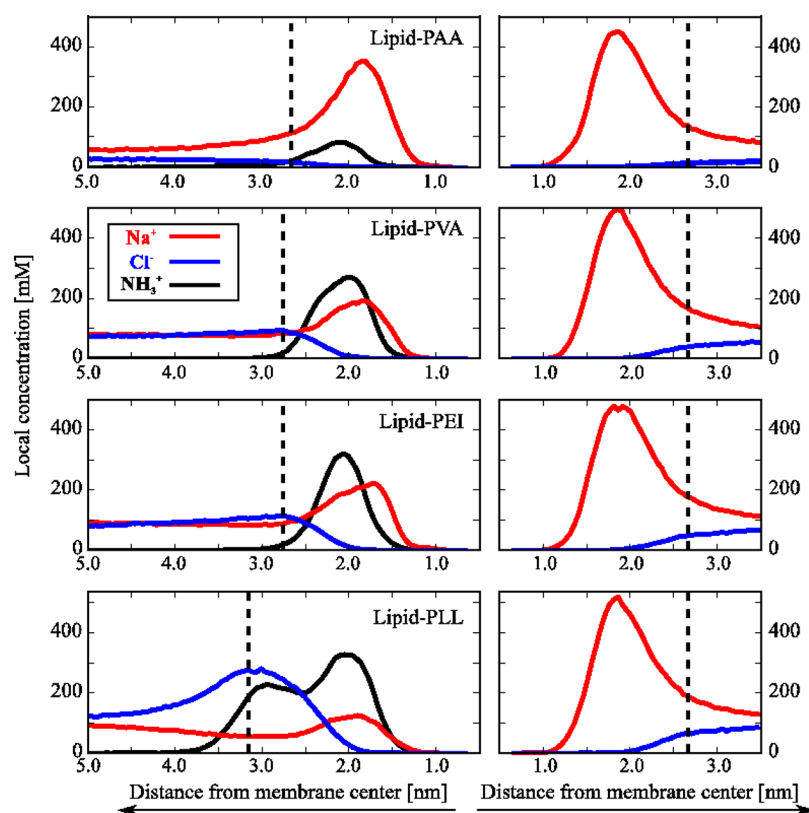


Figure 7. Local concentration of sodium (red line) and chloride (blue line) ions as well as protonated amine groups of polymers (black line) as a function of the distance from the membrane center ($z = 0$). To fit the same scale, the concentration of protonated amine groups was reduced by a factor of 2. The position of the outer Helmholtz plane is shown by a dashed line on both sides of the membrane.

in membrane systems to anionic or anion/zwitterionic lipid compositions.^{69,70} It turns out that the PEI(PVA)-induced overcharging can be observed only under the assumption that binding centers of a polycation and adsorbed sodium ions are independent (adsorption of a polycation is assumed to be irreversible), see Figure 8 (top). What is more, the contribution of Na^+ ions to the surface charge systematically drops with an increase in polymer's charge but never vanishes as evident from Figure 8 (bottom). Therefore, the observed overcharging of a PE/PG membrane by PEI and PVA is most likely a cooperative effect of a polycation and sodium ions. The theoretical dependence of the surface potential on the polymer contribution to the surface charge (Figure 8 (top)) can further be validated experimentally through the measurement of the ζ -potential in liposome suspensions. We note that the surface overcharging (or the charge reversal) was also reported in a number of studies on adsorption of polyelectrolytes on oppositely charged surfaces,⁷¹ providing thereby a support to our findings.

In order to characterize the partitioning of polycations into the lipid/water interface, in Figure 6 (bottom), we presented mass density profiles of cationic polymers after initial adsorption has taken place. An approximate position of the water/lipid interface was defined as a point where mass density profiles of lipids and water cross (shown as a dashed line in Figure 6 (bottom)). First of all, the mass density peaks of all polycations are on the right-hand-side from the lipid/water interface, i.e., closer to the water phase, which comes as no surprise as the polymers are charged and the membrane interior is essentially hydrophobic. The mass density peaks of PVA and PEI are considerably closer to the membrane center as

compared to PLL most likely due to a larger overall charge and a more extended architecture (relatively long side chains) of PLL. In turn, the total charge of PAA turns out to be too small to bind tightly to the membrane surface, so that the corresponding mass density peak is much closer to the water phase as compared to PEI and PVA. To this end, it is important to recall that the protonated amine groups of all polycations are located approximately at the same distance from the membrane center (see Figure 7). Interestingly, PAA demonstrates the deepest permeation into the membrane interior among the polycations (up to 1 nm from the membrane center, see Figure 6 (bottom)): the protonation level of PAA is only 15%, its main chain has an uncharged end fragment of 6 monomers (12 hydrocarbons) and correspondingly demonstrates considerable affinity to lipid acyl tails. Thus, the partitioning of polycations into the lipid/water interface is an interplay between the overall charge of a polymer and its hydrophobicity. The former is responsible for the stability of binding, the latter defines an ability to permeate into the lipid core.

To conclude this section, it has to be emphasized that for all polymers the adsorption of a polycation did not affect to a significant extend the membrane's structural characteristics such as the area per lipid, the ordering of lipid hydrocarbon chains, and the membrane roughness.⁶⁶ Furthermore, we did not find any noticeable changes in the structure of polymers upon adsorption. All these findings represent an evidence that the interactions between the membrane and the polycation in our case is relatively weak.

Lateral Organization and Mobility of Lipids. Many experimental studies have clearly demonstrated that adsorption of cationic polymers on membranes that contain anionic lipid

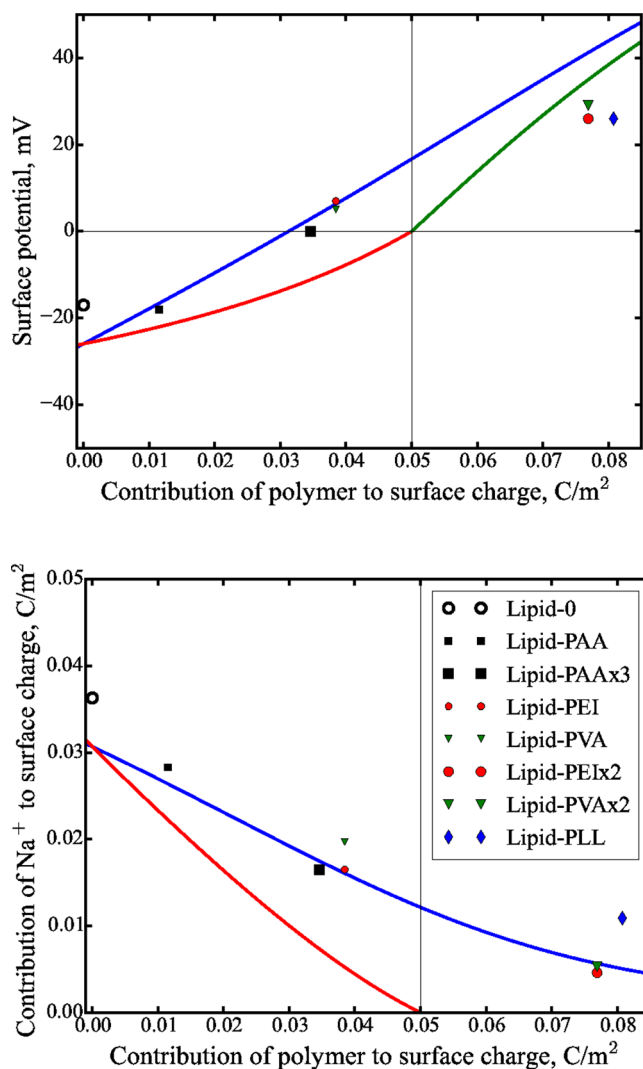


Figure 8. (Top) Surface potential, Ψ_s , as a function of the contribution of a polymer to the surface charge, σ_p . (Bottom) Contribution of sodium ions to the surface charge versus the polymer contribution, σ_p . Theoretical results are shown by lines (blue line corresponds to eq S8, i.e., to independent binding centers; green and red lines are for the situation when a polymer and ions compete for binding sites (eq S9), see the Supporting Information), while computational results are presented by symbols.

species resulted in lipid segregation.^{29–34,72,73} To explore possible polycation-induced lateral reorganization of phospholipids in our simulations, we calculated two-dimensional radial distribution function (2D RDF) for centers of mass of different lipids. In Figure 9, the two-dimensional RDFs are shown for PE–PE and PG–PG pairs. First off, one can see that adsorption of polycations does not affect the lateral distribution of zwitterionic DOPE lipids; see Figure 9 (top). This finding is in line with the above-mentioned fact that polycations interact mostly with head groups of anionic DOPG lipids. In contrast, cationic polymers do affect the distribution of DOPG lipids, the effect being different for polycations of different types. In particular, adsorption of PVA and PEI results in a noticeable lateral redistribution of DOPG lipid molecules as evident from the appearance of clear peaks in 2D RDFs (see Figure 9 (bottom)), which is a sign of the ordering of PG lipids on the PE/PG membrane surface. Taking the height of the 2D RDF as a measure of the degree of lipid segregation, one can conclude

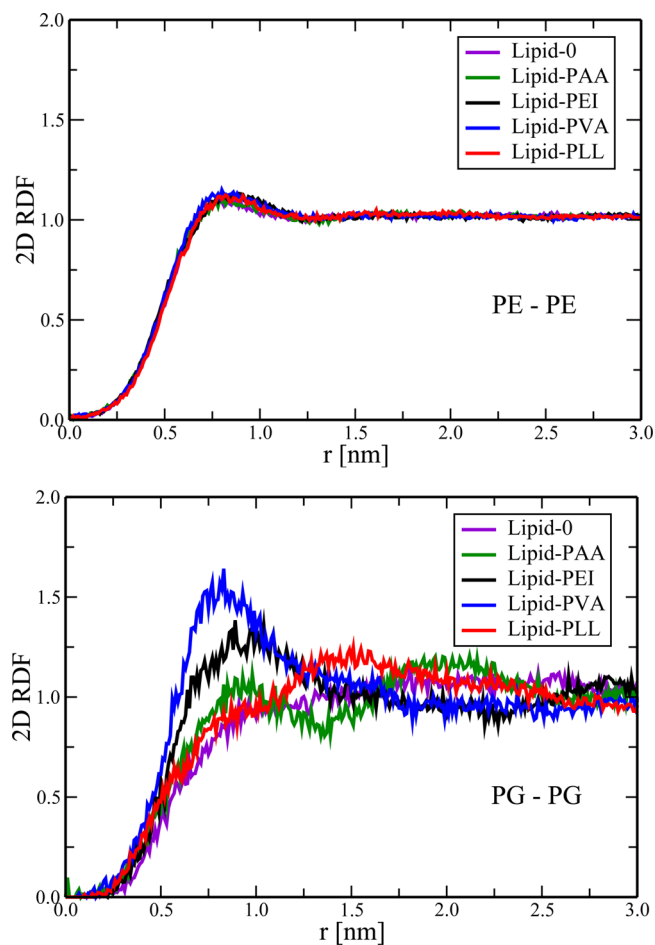


Figure 9. Two-dimensional radial distribution functions of DOPE–DOPE (top) and DOPG–DOPG (bottom) lipids.

that the effect is most pronounced in case of PVA. In turn, as seen from Figure 9 (bottom), adsorption of PAA and PLL has almost no effect on 2D RDFs of PG lipids and correspondingly does not induce lipid segregation.

Another important characteristic that can shed light into the polymer-induced aggregation of anionic lipids is a 2D RDF for lipid molecules and the centers of mass of polycations; see Figure 10. Remarkably, both PEI and PVA accumulate anionic PG lipids as evident through clear RDF peaks in Figure 10 (bottom); the process of PG accumulation is accompanied by depletion of zwitterionic PE lipids in the vicinity of the polycations; see Figure 10 (top). In contrast, PAA and PLL again do not affect the “lipid–polymer” 2D RDFs, demonstrating thereby the above-mentioned lack of lipid aggregation. For PAA this can be explained solely by a very weak binding of a polymer chain to the membrane surface and correspondingly to anionic lipids. However, for a highly charged and tightly bound polycation PLL, the situation is not that trivial. For instance, the calculation of 2D RDFs separately for 100 ns blocks shows that in the beginning of simulations PLL induces PG aggregation in a similar fashion as PEI does; see Figure S1. However, after approximately half a microsecond the corresponding RDF peak for PLL becomes considerably smaller, while the peak for PEI does not change much. Thus, lipid segregation for a well-equilibrated PLL–membrane system is indeed negligibly small.

A possible explanation of such behavior of the Lipid–PLL system could be based on a fact that PLL’s protonated groups

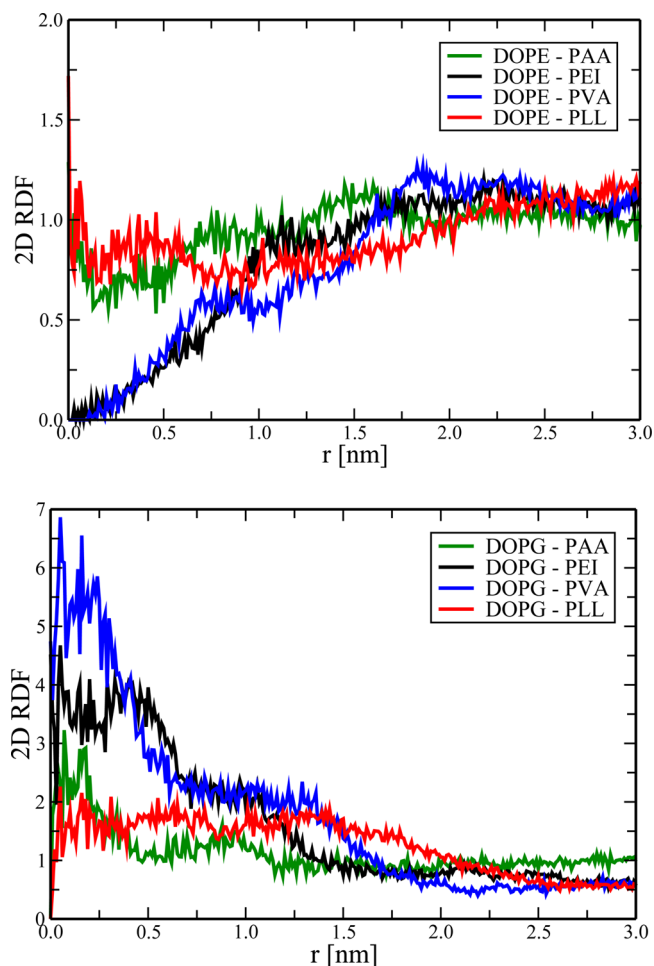


Figure 10. Two-dimensional radial distribution functions of polycation COMs and DOPE (top) and DOPG (bottom) lipids.

bound to the membrane surface are not compact enough. To characterize the compactness of a polycation on the membrane surface, in Figure S2, we plot the 2D radius of gyration for polymer's protonated amine groups that are in contact with anionic PG lipids. As one can see, this characteristic in the case of PLL develops high and frequent spikes, so that DOPG lipids bound to PLL turn out to be considerably less compact as compared to the systems with PEI and PVA. This is most likely due to relatively long PLL side chains that are not able to prevent mixing of anionic and zwitterionic phospholipids under the adsorbed polycation: DOPE lipid molecules can easily fill the space between the PLL-bound DOPG lipids. Visual

inspection of lateral distributions of PE and PG lipids on the membrane surface also confirms this idea; see Figure 11.

Adsorption of polycations to the surface of lipid membranes can affect the lateral mobility of lipid molecules. To characterize possible immobilization effects we calculated the mean-squared displacement (MSD) of lipids in the plane of a membrane. In practice, we split MD trajectories (last 600 ns for the systems with polycations and last 400 for a polycation-free system) into 25 ns pieces. To improve accuracy, for each piece we calculated the MSD of lipids, the overall MSD was evaluated through averaging over all pieces.^{74,75} The resulting MSDs of anionic DOPG lipids are shown in Figure S3. Overall, all the polycations are found to slow down the lateral mobility of anionic lipids. Interestingly, this immobilization is mostly defined by the overall charge of a polycation, so that the effect of a highly charged polycation PLL is most pronounced. As far as zwitterionic DOPE lipids are concerned, adsorption of polycations has almost no effect on their lateral mobility (data not shown).

Polycation Concentration Effects. By far we mostly focused on the impact of a single polycation on the structure and properties of mixed zwitterionic/anionic phospholipid membranes. Increasing concentration of a polycation can be of interest and importance because it allows one to address possible cooperative effects that originate from the presence of several polymer chains in the system. For instance, such cooperativity was proved to be crucial for the ability of antibacterial peptides to induce structural defects (pores) in lipid membranes.^{76–78} Therefore, to explore the polycation concentration effects, we additionally considered membrane systems with multiple polymer chains; see Table 1 for details. The only exception was the Lipid-PLL system as already a single polycation PLL has a charge (+20e) that exceeds considerably the overall charge of a membrane leaflet (−13e).

In Figure S4, we plot mass density profiles of polycations and sodium counterions for the systems with increased polycation concentration. First of all, it is seen that adding several polymer chains in the system does not change the position of peaks of mass density profiles as compared to the systems with a single polycation; see Figure S4 (top). In turn, the height of the peaks increases when the polymer concentration goes up, indicating a noticeable accumulation of polycations on the membrane surface. Therefore, one can witness additivity of contributions of different polymer chains upon adsorption, although one has certain competition between the chains on membrane surface; see Figure S5. It is noteworthy that for PAA such polycation accumulation at the surface also leads to an increased polymer content inside the membrane (on the left-hand side from the lipid/water interface shown by dashed line in Figure S4 (top)).

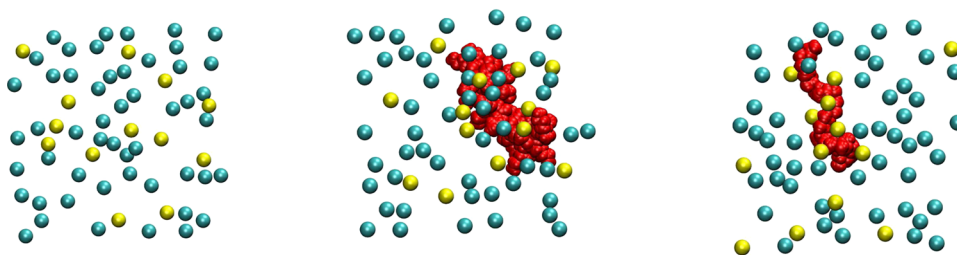


Figure 11. Bottom view on a membrane leaflet to which a polycation is bound. Shown are typical snapshots for a reference polycation-free system (left) and for systems with PLL (middle) and PVA (right). Polycations are shown in red, and phosphorus atoms of DOPE and DOPG lipids are shown in cyan and yellow, respectively; the rest of lipid atoms are not shown.

As far as mass density profiles of sodium counterions are concerned, the above-mentioned additivity of charges of different chains results in much stronger release of Na ions out of the membrane surface; see Figure S4 (bottom). However, not only the overall charge of polycations matters, the polymer geometry is also important. Indeed, in spite of the fact that the total charge of cationic polymers in systems Lipid-PVA \times 2 and Lipid-PEI \times 2 is approximately the same as the charge in the Lipid-PLL system, pairs of PVA and PEI chains cover the membrane surface in a more effective way as compared to a single PLL, resulting in an almost complete release of counterions; see Figure S4 (bottom).

The progressive accumulation of polycation charges upon an increase in polymer concentration is also seen in the reorientation of water molecules nearby the lipid/water interface. Now not only a PLL chain but also pairs of PVA/PEI chains induce the inverted reorientation of water dipoles close to the lipid/water interface; see Figure S6. In contrast to a single-chain situation, three copies of PAA (the overall charge of $+9e$) can neutralize the membrane surface charge to some extent, although their cumulative effect is weaker than the one induced by a single PEI/PVA chain, highlighting the importance of the stability of adsorption as well as the ability of dense covering of the membrane surface.

When considering 2D RDFs of PG–PG pairs for the systems with increased polymer concentration, one can notice an interesting difference from what was seen for the systems with single polycation chains: the 2D RDF peak for PEI increases with polymer concentration, while the corresponding peak for PVA demonstrates an opposite trend; see Figures 12 (top) and 9 (bottom). The same effect is also seen for 2D RDFs of DOPG and the centers of mass of polycations; see Figures 12 (bottom) and 10 (bottom). A possible explanation of this intriguing difference can be found in Figure 4 (bottom) where we plot the numbers of contacts (per polymer chain) between protonated amine groups of polymers and phosphate groups of anionic DOPG lipids. A comparison with single-polymer systems (Figure 4 (top)) shows that the increased polymer concentration does not affect much the number of contacts for PEI but almost halves those for PVA. Indeed, averaging over last 600 ns gives 5 ± 1 and 3 ± 1 contacts per chain for systems Lipid-PEI \times 2 and Lipid-PVA \times 2, respectively, while one has 7 ± 2 and 6 ± 2 for systems Lipid-PEI and Lipid-PVA. This implies that due to stronger binding to anionic lipids two PVA chains compete with each other for binding sites, hindering lipid aggregation around individual chains. In turn, weaker interactions with anionic lipids allows PEI chains to bind almost independently to the membrane surface, following closely the above-mentioned additivity pattern. It is also worth to note that a more flexible nature of PEI chains could contribute to the observed difference.

Finally, we studied the effects of polymer concentration on the lateral mobility of anionic DOPG lipids. As seen from Figure S7, the larger the accumulated charge is, the stronger immobilization of lipids is observed, in line with the results found for single-polymer systems.

CONCLUSIONS

While synthetic cationic polymers are known to be effective as antibacterial agents, the molecular mechanisms behind their antimicrobial activity remain poorly understood. To address this problem, here we employ atomic-scale molecular dynamics simulations to systematically explore adsorption of linear

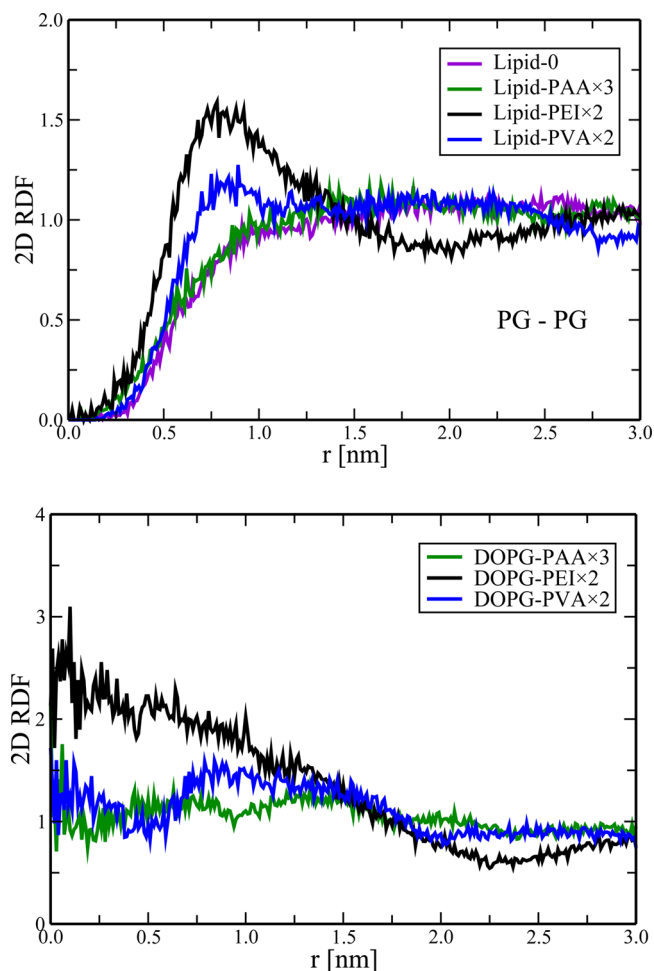


Figure 12. Two-dimensional radial distribution functions of DOPG–DOPG lipids (top) and polycation COMs and DOPG lipids (bottom) for membrane systems with multiple polymer chains.

cationic polymers from aqueous solution on a model bacterial membrane that consists of a 4:1 mixture of zwitterionic DOPE and anionic DOPG lipids. The following four linear polycations are considered: polyallylamine (PAA), polyethylenimine (PEI), polyvinylamine (PVA), and poly-L-lysine (PLL). These polymers differ in their chemical structure: PAA and PVA have a more hydrophobic (hydrocarbon) main chain, while PEI and PLL have amine groups in their backbones main chains; all the polymers except PEI have side chains of various lengths; see Figure 1. Furthermore, the polycations are in different protonation states at physiological conditions (pH 7), and their overall charges are listed in Table 1. We note that, to the best of our knowledge, interactions of PAA and PVA with model biological membranes have never been studied with the use of atomistic MD simulations.

Overall, our computational findings show that the impact of cationic polymers on a model phospholipid PE/PG membrane is mainly determined by the overall electric charge of a polymer. In particular, the process of initial polycation binding to the membrane surface as well as the stability of the binding is governed by the total polymer charge: the larger polycation's protonation level, the tighter binding to the membrane surface. Therefore, the stability of binding increases from PAA (protonation level 15%) via PEI and PVA (both 50%) to PLL (100%). A polymer charge is also responsible for

adsorption-induced changes in the water/lipid interface. Binding of polycations to the negatively charged membrane surface effectively neutralizes its charge, leading to the reorientation of water molecules close to the interface and to the release of counterions of anionic lipids to the water phase. Nevertheless, the counterions are shown to always contribute to the surface charge as, according to the Gouy–Chapman–Stern theory, they do not compete with the polymer for binding centers. This is the reason why we observed a polymer-induced overcharging of an anionic phospholipid membrane even in the case when the overall charge of the polymer is smaller than that of the membrane leaflet. What is more, electrostatic attractive interactions and hydrogen bonding between protonated amine groups of polymers and head groups of anionic PG lipids represent main factors responsible for the stability of the resulting “polycation–membrane” complex: even after polycation’s adsorption has taken place, polymers still interact preferably with anionic PG lipids in spite of the fact that the number of zwitterionic PE lipids is four times larger than that for anionic ones. Another major effect of polycation adsorption is in immobilization of anionic lipids on the membrane surface, the drop in the lateral mobility of lipids being more pronounced when polymer species of a considerable charge are bound to the membrane.

In addition to the above results, we found that some of polycation-induced changes in the properties of membranes are defined not only by the overall charge of a cationic polymer but also by the polymer architecture. In particular, PVA and PEI are shown to accumulate anionic PG lipids on the membrane surface, leading to lipid segregation. In turn, a cationic polymer PLL, whose charge twice exceeds charges of PVA/PEI, does not induce such lipid segregation due to its considerably less compact architecture and relatively long side chains. We note that this computational finding is in line with experimental data that showed that short PLL chains are not able to induce phase separation in neutral/anionic lipid mixtures.³² Another important effect of a polycation is its partitioning into the lipid/water interface as it can directly be related to the ability of a polycation to induce structural defects in the membrane. Interestingly, a cationic polymer PAA that has the smallest overall charge showed the deepest permeation into the lipid/water interface. However, its impact is limited by a rather unstable binding to the membrane due to insufficient protonation. Therefore, the partitioning of a polycation into the lipid/water interface is most likely an interplay between its protonation level (the overall charge) and hydrophobicity of a polymer. Tuning these polycations’ properties via proper combination of protonated and hydrophobic blocks could be one of the possible strategies for constructing highly efficient antimicrobial polymeric agents.

■ ASSOCIATED CONTENT

■ Supporting Information

The Supporting Information is available free of charge on the ACS Publications website at DOI: 10.1021/acs.langmuir.6b02593.

Gouy–Chapman–Stern theory for adsorption of polycations on anionic lipid membranes; additional results for the membrane systems with single and multiple polycation chains (PDF)

■ AUTHOR INFORMATION

Corresponding Author

*E-mail: agurtovenko@gmail.com. Web: www.biosimu.org. Phone: +7-812-3285601. Fax: +7-812-3286869.

Notes

The authors declare no competing financial interest.

■ ACKNOWLEDGMENTS

The authors wish to acknowledge the use of the computer cluster of the Institute of Macromolecular Compounds RAS, the Lomonosov supercomputer at the Moscow State University and computers of the Sector of Mathematical Biophysics of Complex Systems (Faculty of Biology, Lomonosov Moscow State University). Authors also thank Alexander Kolsanov, Boris Yaremin, and Vladimir Gusev from the Samara State Medical University for access to the computational facilities of PACS “LUCH-S”. This work was partly supported by the Presidium of the Russian Academy of Sciences through the grant program “Molecular and Cellular Biology”, by the St. Petersburg State University (Grant 11.37.290.2015), and by the Russian Foundation for Basic Research (No. 16-04-00556a).

■ REFERENCES

- (1) Kenawy, E.-R.; Worley, S. D.; Broughton, R. The Chemistry and Applications of Antimicrobial Polymers: A State-of-the-Art Review. *Biomacromolecules* **2007**, *8*, 1359–1384.
- (2) Munoz-Boñilla, A.; Fernández-García, M. Polymeric Materials with Antimicrobial Activity. *Prog. Polym. Sci.* **2012**, *37*, 281–339.
- (3) Tyagi, P. K.; Gupta, B.; Singh, H. Radiation-Induced Grafting of 2-Hydroxyethyl Methacrylate onto Polypropylene for Biomedical Applications. 2. Evaluation as Antimicrobial Suture. *J. Macromol. Sci., Part A: Pure Appl. Chem.* **1993**, *A30*, 303–313.
- (4) Imazato, S.; Ebi, N.; Takahashi, Y.; Kaneko, T.; Ebisu, S.; Russell, R. Antibacterial Activity of Bactericide-Immobilized Filler for Resin-Based Restoratives. *Biomaterials* **2003**, *24*, 3605–3609.
- (5) Kenawy, E.-R.; Abdel-Hay, F. I.; El-Shanshoury, A. E.-R.; El-Newehy, M. H. Biologically Active Polymers. V. Synthesis and Antimicrobial Activity of Modified Poly(glycidyl methacrylate-co-2-hydroxyethyl methacrylate) Derivatives with Quaternary Ammonium and Phosphonium Salts. *J. Polym. Sci., Part A: Polym. Chem.* **2002**, *40*, 2384–2393.
- (6) Tan, S.; Li, G.; Shen, J.; Liu, Y.; Zong, M. J. Study of Modified Polypropylene Nonwoven Cloth. II. Antibacterial Activity of Modified Polypropylene Nonwoven Cloths. *J. Appl. Polym. Sci.* **2000**, *77*, 1869–1876.
- (7) Li, G.; Shen, J. J. A Study of Pyridinium-Type Functional Polymers. IV. Behavioral Features of the Antibacterial Activity of Insoluble Pyridinium-Type Polymers. *J. Appl. Polym. Sci.* **2000**, *78*, 676–684.
- (8) Arora, S.; Yadav, V.; Kumar, P.; Gupta, R.; Kumar, D. Polymer Based Antimicrobial Coatings as Potential Biomaterial: A Review. *Int. J. Pharm. Sci. Rev. Res.* **2013**, *23*, 279–290.
- (9) Lin, J.; Tiller, J. C.; Lee, S. B.; Lewis, K.; Klivanov, A. M. Insights into Bactericidal Action of Surface-Attached Poly(vinyl-N-hexylpyridinium) Chains. *Biotechnol. Lett.* **2002**, *24*, 801–805.
- (10) Ikeda, T.; Yamaguchi, H.; Tazuke, S. New Polymeric Biocides: Synthesis and Antibacterial Activities of Polycations with Pendant Biguanide Groups. *Antimicrob. Agents Chemother.* **1984**, *26*, 139–144.
- (11) Kanazawa, A.; Ikeda, T.; Endo, T. Novel Polycationic Biocides: Synthesis and Antibacterial Activity of Polymeric Phosphonium Salts. *J. Polym. Sci., Part A: Polym. Chem.* **1993**, *31*, 335–343.
- (12) Helander, I. M.; Alakomi, H.-L.; Latva-Kala, K.; Koski, P. Polyethyleneimine is an Effective Permeabilizer of Gram-Negative Bacteria. *Microbiology* **1997**, *143*, 3193–3199.

- (13) Lin, J.; Qiu, S.; Lewis, K.; Klivanov, A. M. Bactericidal Properties of Flat Surfaces and Nanoparticles Derivatized with Alkylated Polyethylenimines. *Biotechnol. Prog.* **2002**, *18*, 1082–1086.
- (14) Panarin, E. F.; Solovskii, M. V.; Zaikina, N. A.; Afinogenov, G. E. Biological Activity of Cationic Polyelectrolytes. *Makromol. Chem.* **1985**, *9*, 25–33.
- (15) Westman, E.-H.; Ek, M.; Enarsson, L.-E.; Wågberg, L. Assessment of Antibacterial Properties of Polyvinylamine (PVAm) with Different Charge Densities and Hydrophobic Modifications. *Biomacromolecules* **2009**, *10*, 1478–1483.
- (16) Illergård, J.; Römling, U.; Wågberg, L.; Ek, M. Biointeractive Antibacterial Fibres Using Polyelectrolyte Multilayer Modification. *Cellulose* **2012**, *19*, 1731–1741.
- (17) Wyrwal, M.; Koczurkiewicz, P.; Wójcik, K.; Michalik, M.; Kozik, B.; Żylewski, M.; Nowakowska, M.; Kepczynski, M. Synthesis of Strong Polycations with Improved Biological Properties. *J. Biomed. Mater. Res., Part A* **2014**, *102A*, 721–731.
- (18) Iarikov, D. D.; Kargar, M.; Sahari, A.; Russel, L.; Gause, K. T.; Behkam, B.; Ducker, W. A. A. Antimicrobial Surfaces using Covalently Bound Polyallylamine. *Biomacromolecules* **2014**, *15*, 169–176.
- (19) Vaara, M.; Vaara, T. Polycations as Outer Membrane-Disorganizing Agents. *Antimicrob. Agents Chemother.* **1983**, *24*, 114–122.
- (20) Shima, S.; Matsuoka, H.; Iwamoto, T.; Sakai, H. Antimicrobial Action of *ε*-Poly-L-Lysine. *J. Antibiot.* **1984**, *37*, 1449–1455.
- (21) Shai, Y. Mechanism of the Binding, Insertion and Destabilization of Phospholipid Bilayer Membranes by Alpha-Helical Antimicrobial and Cell Non-Selective Membrane-Lytic Peptides. *Biochim. Biophys. Acta, Biomembr.* **1999**, *1462*, 55–70.
- (22) Blondelle, S. E.; Lohner, K.; Aguilar, M.-I. Lipid-Induced Conformation and Lipid-Binding Properties of Cytolytic and Antimicrobial Peptides: Determination and Biological Specificity. *Biochim. Biophys. Acta, Biomembr.* **1999**, *1462*, 89–108.
- (23) Guzmán, F.; Marshall, S.; Ojeda, C.; Albericio, F.; Carvajal-Rondanelli, P. Inhibitory Effect of Short Cationic Homopeptides against Gram-Positive Bacteria. *J. Pept. Sci.* **2013**, *19*, 792–800.
- (24) Timofeeva, L.; Kleshcheva, N. Antimicrobial Polymers: Mechanism of Action, Factors of Activity, and Applications. *Appl. Microbiol. Biotechnol.* **2011**, *89*, 475–492.
- (25) Schulz, M.; Olubummo, A.; Binder, W. H. Beyond the Lipid-Bilayer: Interaction of Polymers and Nanoparticles with Membranes. *Soft Matter* **2012**, *8*, 4849–4864.
- (26) Rossi, G.; Monticelli, L. Modeling the Effect of Nano-Sized Polymer Particles on the Properties of Lipid Membranes. *J. Phys.: Condens. Matter* **2014**, *26*, 503101.
- (27) Ikeda, T.; Tazuke, S.; Watanabe, M. Interaction of Biologically Active Molecules with Phospholipid Membranes I. Fluorescence Depolarization Studies on the Effect of Polymeric Biocide Bearing Biguanide Groups in the Main Chain. *Biochim. Biophys. Acta, Biomembr.* **1983**, *735*, 380–386.
- (28) Ikeda, T.; Ledwith, A.; Bamford, C. H.; Hann, R. A. Interaction of a Polymeric Biguanide Biocide with Phospholipid Membranes. *Biochim. Biophys. Acta, Biomembr.* **1984**, *769*, 57–66.
- (29) Yaroslavov, A. A.; Efimova, A. A.; Sybachin, A. V. Effect of the Phase State of the Lipid Bilayer on the Structure and Characteristics of the Polycation-(Anionic Liposome) Complex. *Polym. Sci., Ser. A* **2009**, *51*, 638–647.
- (30) Macdonald, P. M.; Crowell, K. J.; Franzin, C. M.; Mitroskos, P.; Semchyschyn, D. J. ²H NMR and Polyelectrolyte-Induced Domains in Lipid Bilayers. *Solid State Nucl. Magn. Reson.* **2000**, *16*, 21–36.
- (31) Franzin, C. M.; Macdonald, P. M. Polylysine-Induced ²H NMR-Observable Domains in Phosphatidylserine/Phosphatidylcholine Lipid Bilayers. *Biophys. J.* **2001**, *81*, 3346–3362.
- (32) Laroche, C.; Carrier, D.; Pezolet, M. Study of the Effect of Poly(L-Lysine) on Phosphatidic Acid and Phosphatidylcholine/Phosphatidic Acid Bilayers by Raman Spectroscopy. *Biochemistry* **1988**, *27*, 6220–6228.
- (33) Carrier, D.; Pezolet, M. Investigation of Polylysine-Dipalmitoylphosphatidylglycerol Interactions in Model Membranes. *Biochemistry* **1986**, *25*, 4167–4174.
- (34) Schwieger, C.; Blume, A. Interaction of Poly(L-Lysines) with Negatively Charged Membranes: An FT-IR and DSC Study. *Eur. Biophys. J.* **2007**, *36*, 437–450.
- (35) Oku, N.; Yamaguchi, N.; Shibamoto, S.; Ito, F.; Nango, M. The Fusogenic Effect of Synthetic Polycations on Negatively Charged Lipid Bilayers. *J. Biochem.* **1986**, *100*, 935–944.
- (36) Tian, W. D.; Ma, Y. Q. Theoretical and Computational Studies of Dendrimers as Delivery Vectors. *Chem. Soc. Rev.* **2013**, *42*, 705–727.
- (37) Kepczynski, M.; Jamroz, D.; Wyrwal, M.; Bednar, J.; Rząd, E.; Nowakowska, M. Interactions of a Hydrophobically Modified Polycation with Zwitterionic Lipid Membranes. *Langmuir* **2012**, *28*, 676–688.
- (38) Hill, E. H.; Stratton, K.; Whitten, D. G.; Evans, D. G. Molecular Dynamics Simulation Study of the Interaction of Cationic Biocides with Lipid Bilayers: Aggregation Effects and Bilayer Damage. *Langmuir* **2012**, *28*, 14849–14854.
- (39) Hill, E. H.; Whitten, D. G.; Evans, D. G. Computational Study of Bacterial Membrane Disruption by Cationic Biocides: Structural Basis for Water Pore Formation. *J. Phys. Chem. B* **2014**, *118*, 9722–9732.
- (40) Choudhury, C. K.; Kumar, A.; Roy, S. Characterization of Conformation and Interaction of Gene Delivery Vector Polyethylenimine with Phospholipid Bilayer at Different Protonation State. *Biomacromolecules* **2013**, *14*, 3759–3768.
- (41) Lorenz, C. D.; Faraudo, J.; Traveset, A. Hydrogen Bonding and Binding of Polybasic Residues with Negatively Charged Mixed Lipid Monolayers. *Langmuir* **2008**, *24*, 1654–1658.
- (42) Gurtovenko, A. A.; Anwar, J.; Vattulainen, I. Defect-Mediated Trafficking across Cell Membranes: Insights from In Silico Modeling. *Chem. Rev.* **2010**, *110*, 6077–6103.
- (43) Eband, R. F.; Savage, P. B.; Eband, R. M. Bacterial Lipid Composition and the Antimicrobial Efficacy of Cationic Steroid Compounds (Ceragenins). *Biochim. Biophys. Acta, Biomembr.* **2007**, *1768*, 2500–2509.
- (44) Wang, Y.; Tang, Y.; Zhou, Z.; Ji, E.; Lopez, G. P.; Chi, E. Y.; Schanze, K. S.; Whitten, D. G. Membrane Perturbation Activity of Cationic Phenylene Ethynylene Oligomers and Polymers: Selectivity against Model Bacterial and Mammalian Membranes. *Langmuir* **2010**, *26*, 12509–12514.
- (45) Zhao, W.; Róg, T.; Gurtovenko, A. A.; Vattulainen, I.; Karttunen, M. Role of Phosphatidylglycerols in the Stability of Bacterial Membranes. *Biochimie* **2008**, *90*, 930–938.
- (46) Suh, J.; Paik, H.-J.; Hwang, B. K. Ionization of Poly(ethylenimine) and Poly(allylamine) at Various pH's. *Bioorg. Chem.* **1994**, *22*, 318–327.
- (47) Smits, R. G.; Koper, G. J. M.; Mandel, M. The Influence of Nearest- and Next-Nearest-Neighbor Interactions on the Potentiometric Titration of Linear Poly(ethylenimine). *J. Phys. Chem.* **1993**, *97*, 5745–5751.
- (48) Katchalsky, A.; Mazur, J.; Spitnik, P. Polybase Properties of Polyvinylamine. *J. Polym. Sci.* **1957**, *23*, 513–532.
- (49) Jämbeck, J. P. M.; Lyubartsev, A. P. Derivation and Systematic Validation of a Refined All-Atom Force Field for Phosphatidylcholine Lipids. *J. Phys. Chem. B* **2012**, *116*, 3164–3179.
- (50) Jämbeck, J. P. M.; Lyubartsev, A. P. An Extension and Further Validation of an All-Atomistic Force Field for Biological Membranes. *J. Chem. Theory Comput.* **2012**, *8*, 2938–2948.
- (51) Jämbeck, J. P. M.; Lyubartsev, A. P. Another Piece of the Membrane Puzzle: Extending Slipids Further. *J. Chem. Theory Comput.* **2013**, *9*, 774–784.
- (52) Joung, I. S.; Cheatham, T. E. Determination of Alkali and Halide Monovalent Ion Parameters for Use in Explicitly Solvated Biomolecular Simulations. *J. Phys. Chem. B* **2008**, *112*, 9020–9041.

- (53) Jorgensen, W. L.; Chandrasekhar, J.; Madura, J. D.; Impey, R. W.; Klein, M. L. Comparison of Simple Potential Functions for Simulating Liquid Water. *J. Chem. Phys.* **1983**, *79*, 926–935.
- (54) Wang, J.; Cieplak, P.; Kollman, P. A. How Well Does a Restrained Electrostatic Potential (RESP) Model Perform in Calculating Conformational Energies of Organic and Biological Molecules? *J. Comput. Chem.* **2000**, *21*, 1049–1074.
- (55) Sorin, E. J.; Pande, V. S. Exploring the Helix-Coil Transition via All-Atom Equilibrium Ensemble Simulations. *Biophys. J.* **2005**, *88*, 2472–2493.
- (56) Kondinskaia, D. A.; Kostritskii, A. Y.; Nesterenko, A. M.; Antipina, A. Y.; Gurtovenko, A. A. Atomic-Scale Molecular Dynamics Simulations of DNA-Polycation Complexes: Two Distinct Binding Patterns. *J. Phys. Chem. B* **2016**, *120*, 6546–6554.
- (57) Hess, B.; Kutzner, C.; van der Spoel, D.; Lindahl, E. GROMACS 4: Algorithms for Highly Efficient, Load-Balanced, and Scalable Molecular Simulation. *J. Chem. Theory Comput.* **2008**, *4*, 435–447.
- (58) Berendsen, H. J. C.; Postma, J. P. M.; van Gunsteren, W. F.; DiNola, A.; Haak, J. R. Molecular Dynamics with Coupling to an External Bath. *J. Chem. Phys.* **1984**, *81*, 3684–3690.
- (59) Nosé, S. A Molecular Dynamics Method for Simulations in the Canonical Ensemble. *Mol. Phys.* **1984**, *52*, 255–268.
- (60) Hoover, W. G. Canonical Dynamics: Equilibrium Phase-Space Distributions. *Phys. Rev. A: At, Mol., Opt. Phys.* **1985**, *31*, 1695–1697.
- (61) Parrinello, M.; Rahman, A. Polymorphic Transitions in Single Crystals: A New Molecular Dynamics Method. *J. Appl. Phys.* **1981**, *52*, 7182–7190.
- (62) Hess, B.; Bekker, H.; Berendsen, H. J. C.; Fraaije, J. G. E. M. LINCS: A Linear Constraint Solver for Molecular Simulations. *J. Comput. Chem.* **1997**, *18*, 1463–1472.
- (63) Essmann, U.; Perera, L.; Berkowitz, M. L.; Darden, T.; Lee, H.; Pedersen, L. G. A Smooth Particle Mesh Ewald Method. *J. Chem. Phys.* **1995**, *103*, 8577–8592.
- (64) Humphrey, W.; Dalke, A.; Schulten, K. VMD - Visual Molecular Dynamics. *J. Mol. Graphics* **1996**, *14*, 33–38.
- (65) Nesterenko, A. M.; Ermakov, Y. A. Molecular-Dynamic Simulation of Phospholipid Bilayers: Ion Distribution at the Surface of Neutral and Charged Bilayer in the Liquid Crystalline State. *Biochem. Suppl. Ser. A Membr. Cell Biol.* **2012**, *6*, 320–328.
- (66) Bresme, F.; Faraudo, J. Computer Simulation Studies of Newton Black Films. *Langmuir* **2004**, *20*, 5127–5137.
- (67) Gurtovenko, A. A.; Vattulainen, I. Effect of NaCl and KCl on Phosphatidylcholine and Phosphatidylethanolamine Lipid Membranes: Insight from Atomic-Scale Simulations for Understanding Salt-Induced Effects in the Plasma Membrane. *J. Phys. Chem. B* **2008**, *112*, 1953–1962.
- (68) Antipina, A. Y.; Gurtovenko, A. A. Molecular Mechanism of Calcium-Induced Adsorption of DNA on Zwitterionic Phospholipid Membranes. *J. Phys. Chem. B* **2015**, *119*, 6638–6645.
- (69) McLaughlin, S. Electrostatic potentials at membrane-solution interfaces. In *Current Topics in Membranes and Transport*; Bronner, F., Kleinzeller, A., Eds.; Academic Press: New York, , 1977; Vol. 9, pp 71–144.
- (70) Ermakov, Y. A. The Determination of Binding-Site Density and Association Constants for Monovalent Cation Adsorption onto Liposomes Made from Mixtures of Zwitterionic and Charged Lipids. *Biochim. Biophys. Acta, Biomembr.* **1990**, *1023*, 91–97.
- (71) Faraudo, J.; Martin-Molina, A. Competing Forces in the Interaction of Polyelectrolytes with Charged Interfaces. *Curr. Opin. Colloid Interface Sci.* **2013**, *18*, 517–523.
- (72) Tzilil, S.; Ben-Shaul, A. Flexible Charged Macromolecules on Mixed Fluid Lipid Membranes: Theory and Monte Carlo Simulations. *Biophys. J.* **2005**, *89*, 2972–2987.
- (73) Duan, X.; Zhang, R.; Li, Y.; Shi, T.; An, L.; Huang, Q. Monte Carlo Study of Polyelectrolyte Adsorption on Mixed Lipid Membrane. *J. Phys. Chem. B* **2013**, *117*, 989–1002.
- (74) Gurtovenko, A. A. Asymmetry of Lipid Bilayers Induced by Monovalent Salt: Atomistic Molecular Dynamics Study. *J. Chem. Phys.* **2005**, *122*, 244902.
- (75) Antipina, A. Y.; Gurtovenko, A. A. Molecular-Level Insight into the Interactions of DNA with Phospholipid Bilayers: Barriers and Triggers. *RSC Adv.* **2016**, *6*, 36425–36432.
- (76) Sengupta, D.; Leontiadou, H.; Mark, A. E.; Marrink, S.-J. Toroidal Pores Formed by Antimicrobial Peptides Show Significant Disorder. *Biochim. Biophys. Acta, Biomembr.* **2008**, *1778*, 2308–2317.
- (77) Rzepiela, A.; Sengupta, D.; Goga, N.; Marrink, S.-J. Membrane Poration by Antimicrobial Peptides Combining Atomistic and Coarse-Grained Descriptions. *Faraday Discuss.* **2010**, *144*, 431–443.
- (78) Leontiadou, H.; Mark, A. E.; Marrink, S.-J. Antimicrobial Peptides in Action. *J. Am. Chem. Soc.* **2006**, *128*, 12156–12161.